# Meta-GGA that describes weak interactions in addition to bond energies and band gaps

Timo Lebeda [*] and Stephan Kümmel [†]
*Theoretical Physics IV, University of Bayreuth, 95440 Bayreuth, Germany*

(Received 10 December 2024; revised 18 February 2025; accepted 3 April 2025; published 18 April 2025)

We show that the recently proposed Lebeda-Aschebrock-Kümmel (LAK) meta-generalized gradient approximation, the accuracy of which was previously established for atomization energies, bond lengths, and band gaps, also captures weak interactions near equilibrium without a dispersion correction. We discuss how this is achieved. Furthermore, we show that among the semilocal cost pure functionals, LAK is the one that reaches the highest accuracy for the large GMTKN55 database for general thermochemistry and kinetics. Next, we explain the design strategy of enhancement factor engineering. Its key idea is to complement exact constraints with construction principles. Finally, we discuss areas of research in which the use of LAK may offer advantages over existing functionals.

DOI: 10.1103/PhysRevB.111.155133

## I. INTRODUCTION

For modeling real materials, weak interactions are of considerable importance. In the realm of soft materials, e.g., biological systems, at interfaces, and surfaces, the accurate description of both covalent binding and weak interactions is essential [1]. As such systems typically also comprise a large number of atoms, computational efficiency becomes a critical aspect.

Its attractive balance between accuracy and computational cost made density functional theory (DFT) the workhorse of electronic structure theory. Regarding weak interactions, however, there is a long-standing debate whether ground-state exchange-correlation approximations can and should capture weak interactions [1–15]. In principle, the situation is clear: The exact exchange-correlation functional correctly describes all electron-electron interactions, and thus also weak interactions. However, early and common approximations to the exact functional, such as the local density approximation (LDA), the generalized gradient approximation (GGA), and exact (Hartree-Fock) exchange poorly describe weak interactions. Therefore, these methods are typically combined with additional methods for the explicit treatment of dispersion effects, such as nonlocal density-based functionals [16–18] or *a posteriori* dispersion corrections [19–23]. Alternatives are fully nonlocal functionals, e.g., based on the random phase approximation [24,25]. While conceptually satisfying, they usually come at a steeply increased computational cost.

In this paper we focus on the computationally most efficient exchange-correlation approximations, i.e., the class of semilocal density functionals. The capability of meta-generalized gradient approximations (meta-GGAs) to describe noncovalent interactions [26] has ben attributed to their ability to discriminate between covalent and dispersion interactions through their kinetic energy dependence [27]. Thus, in contrast to the LDA and GGA, the description of dispersion interactions in meta-GGAs can be based on systematic concepts, as meta-GGAs can describe both covalent and dispersive interactions by "seeing" and responding adequately to the different bonding types [27,28]. This allows for an accurate description of short- and intermediate-range van der Waals interactions [13,29]. Of course, semilocal density functionals can not capture the long-range $-C_6/R^6$ decay of the van der Waals attraction that exists even for nonoverlapping electron densities [23,30,31]. This would require a fully nonlocal correlation. In case an accurate description of noncovalent interactions far from equilibrium is important, meta-GGAs that include short- and intermediate-range van der Waals interactions can still benefit from a long-range dispersion correction [12], as is well known from the many successes of dispersion-corrected DFT.

While some authors argue that a proper density functional approximation should not contain *any* dispersion interaction and dispersion should only be captured by a dispersion correction [9,14], many of the frequently and successfully used density functionals today either capture the short- and intermediate-range part of the dispersion interaction [13,29] and are corrected for the long-range part if necessary [12,32], or the density functional is directly designed together with its dispersion correction [33–35]. However, from a fundamental perspective, as well as for practical computations, it is desirable to have the density functional itself treat dispersion interactions as well as possible, just like the exact functional would do.

Here, we show that the recent nonempirical Lebeda-Aschebrock-Kümmel (LAK) meta-GGA [36] captures noncovalent interactions near equilibrium remarkably well. In this article we rationalize this property of the functional by working out what is decisive for the description of weak

[*]Contact author: timo.lebeda@uni-bayreuth.de
[†]Contact author: stephan.kuemmel@uni-bayreuth.de

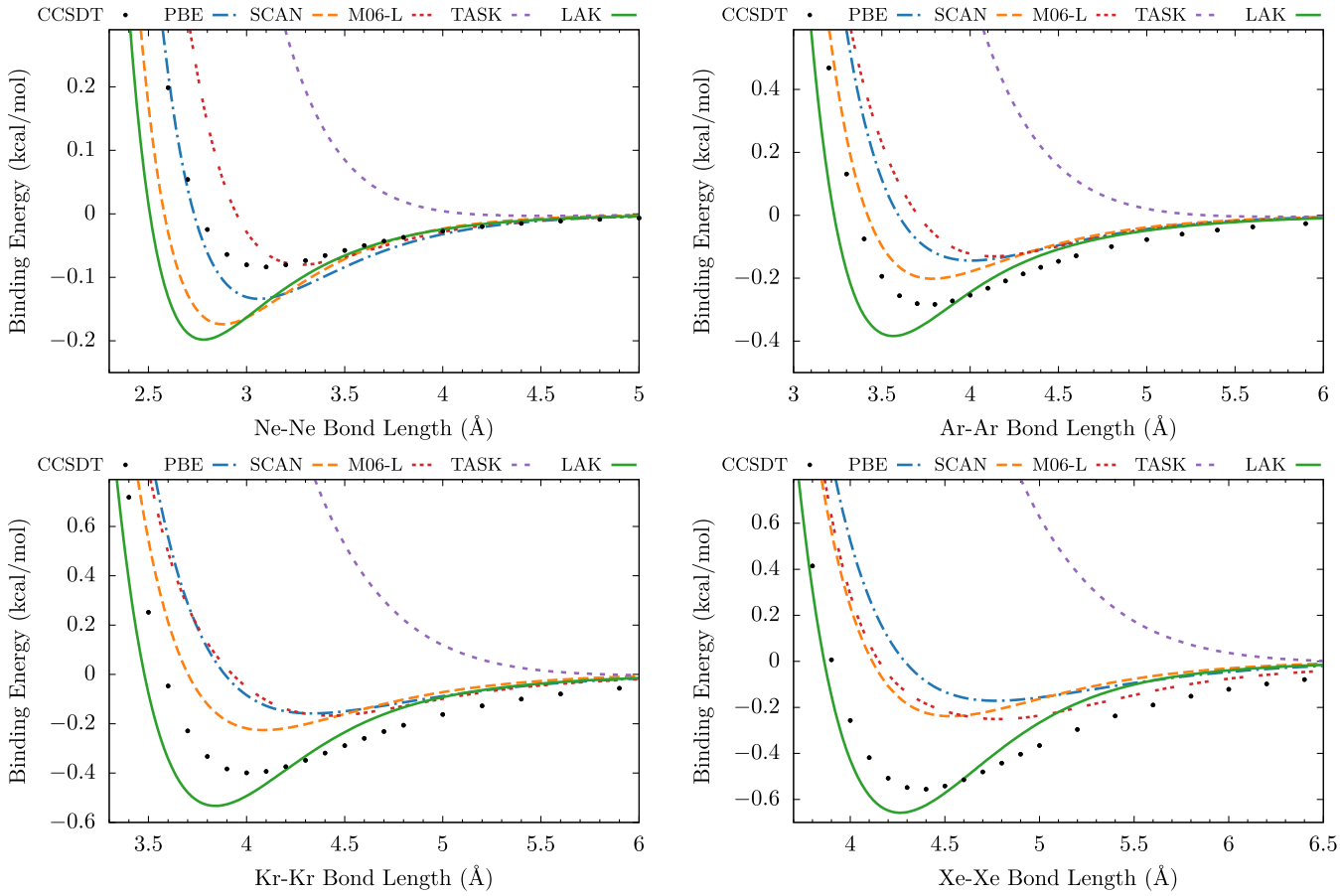


FIG. 1. Rare gas dimer binding curves of LAK compared to selected semilocal density functionals and CCSDT reference values [41–44].

interactions in meta-GGAs. Furthermore, we assess LAK on the large GMTKN55 database for thermochemistry, kinetics, and noncovalent interactions [37]. The results show that LAK is the best pure, semilocal cost density functional on GMTKN55, where pure means without an additional dispersion correction. This demonstrates that LAK manages to describe both covalent and noncovalent interactions with good accuracy from pure DFT. Finally, we discuss the general performance of LAK and outline areas where we consider LAK a possible improvement upon existing functionals.

## II. LAK FOR NONCOVALENT BINDING

We start by directly assessing the LAK functional for a paradigm situation of weak interaction, the binding energy curves of rare gas dimers. Figure 1 shows that LAK captures the van der Waals attraction of rare gas dimers near the equilibrium bond length quite reasonably, and in particularly so for the often challenging heavier atoms. In Fig. 1, we compare the binding curves of $Ne_2$, $Ar_2$, $Kr_2$, and $Xe_2$ for the GGA PBE [38] and the meta-GGAs SCAN [39], M06-L [26], TASK [40], and LAK [36] with highly accurate CCSDT reference data [41–44]. Since $He_2$ is a special case for meta-GGAs, we shortly note that LAK underbinds $He_2$ and defer the discussion of the $He_2$ binding curve to the Supplemental Material [45,46]. Rare gas dimers are well-established model systems for van der Waals interactions [6–8,10,31,47–55] because, first, dispersion interactions are the only source of attraction between rare gas atoms and, second, highly accurate reference data are available for these systems. We compare LAK with PBE, SCAN, and TASK exchange plus LDA correlation (in the parametrization of Perdew and Wang [56]) because they all share the same nonempirical construction philosophy. Additionally, we compare to M06-L [26], because it was the first semilocal density functional for which the capture of noncovalent interactions was systematically explained [27].

All DFT results in this section are obtained from self-consistent all-electron calculations in ADF [57,58] using the QZ4P basis set, the setting EXCELLENT numerical accuracy and a radial grid boost of 3. These extremely fine numerical settings are required to avoid oscillations in the M06-L binding curves [52], and we adopt them for all functionals. However, we should point out that the numerical properties of meta-GGAs depend very much on the details of the construction, and while some meta-GGA are numerically cumbersome, others are as benevolent as GGAs [36,40,59,60].

Figure 1 summarizes the well-known behavior of PBE, M06-L, and SCAN: PBE, while still rather accurate for the $Ne_2$ binding curve, increasingly underestimates the binding with increasing atomic mass. M06-L predicts similar binding curves as PBE for $Ar_2$ and $Kr_2$, but its binding strength relative to PBE increases with the atomic mass. SCAN improves over PBE and M06-L for all systems except $Ne_2$, predicting a larger binding energy near equilibrium and much more accurate equilibrium bond lengths. However, while SCAN is reasonably accurate for the argon dimer, it increasingly

underestimates the binding energy with increasing atomic mass, similar to PBE. This might be due to the use of the compressed argon dimer as one of the "appropriate norms" in the construction of SCAN.

LAK and TASK, whose exchange enhancement factors look formally similar to each other and share the same realization of the gradient expansion of exchange, predict decisively different binding curves: LAK, on the one hand, predicts reasonable binding curves and is remarkably accurate even for the xenon dimer. TASK, on the other hand, predicts no binding at all (or only minimal binding at about twice the CCSDT bond length) and is even more repulsive than exact exchange. This broad spectrum of predictions for weakly bound systems illustrates the delicate sensitivity of the description of weak interactions on details of the meta-GGA construction.

## III. RATIONALIZING NONCOVALENT INTERACTIONS IN META-GGAs

In the following we take a look at how meta-GGAs acquire their sensitivity to noncovalent interactions. Nonempirical meta-GGAs often use the iso-orbital indicator

$$\alpha = \frac{\tau - \tau^W}{\tau^{\text{unif}}}, \tag{1}$$

with the kinetic energy density $\tau = \frac{1}{2}\sum_{j=1}^{N} |\nabla\varphi_j|^2$, its uniform electron gas limit $\tau^{\text{unif}} = (3/10)(3\pi^2)^{2/3} n^{5/3}$, and its iso-orbital limit $\tau^W = |\nabla n|^2/(8n)$. Here, $\{\phi_j\}$ denote the (generalized) Kohn-Sham orbitals, $n = \sum_{j=1}^{N} |\phi_j|^2$ is the electron density, and we use atomic units throughout. Since we only consider spin-unpolarized systems in this section, we suppress spin indices in the notation.

Using $\alpha$ as the kinetic-energy-dependent variable has the advantage that it can discriminate between iso-orbital regions ($\alpha = 0$), uniform densities ($\alpha = 1$), and regions of density overlap between closed shells ($\alpha \gg 1$) [28]. Consequently, covalent bonds have small $\alpha$ at the middle of the bond, whereas dispersive bonds have large $\alpha$.

Besides $n$ and $\alpha$, the exchange energy of a meta-GGA depends on the reduced density gradient $s = |\nabla n|/[2(3\pi^2)^{1/3} n^{4/3}]$ in the form

$$E_{\text{x}}[n] = A_{\text{x}} \int n^{4/3} F_{\text{x}}(s, \alpha) d^3 r, \tag{2}$$

where the exchange enhancement factor $F_{\text{x}}$ is the local enhancement of the exchange energy density over the exchange energy density of a uniform electron gas, $e_{\text{x}}^{\text{unif}} = A_{\text{x}} n^{4/3}$ with $A_{\text{x}} = -(3/4)(3/\pi)^{1/3}$. Consequently, regions of $F_{\text{x}} > 1$ correspond to a locally enhanced exchange energy density and are energetically favored, whereas regions of $F_{\text{x}} < 1$ correspond to a lower local exchange energy density and are energetically suppressed. Similarly, the enhancement factor of exchange and correlation together, $F_{\text{xc}}$, is defined by

$$E_{\text{xc}}[n] = A_{\text{x}} \int n^{4/3} F_{\text{xc}}(r_s, s, \alpha)\, d^3 r, \tag{3}$$

with the Wigner-Seitz radius $r_s = (4\pi n/3)^{-1/3}$.

The mechanisms of how and to what extent GGAs can model noncovalent interactions have been discussed in the literature [3,47,61–63]. However, little is known for meta-GGAs. While the ability of $\alpha$ to recognize regions of noncovalent bonds is well established [27,28], the influence of $\alpha$ on the description of noncovalent interactions is not yet clear [64]. Thus, to understand noncovalent interactions in meta-GGAs, especially with respect to the $\alpha$ dependence, we compare the (exchange) enhancement factors of SCAN, TASK, and LAK in Fig. 2.

For the sake of transparency we first base the following arguments on only the exchange part of the functionals. However, it is clear that only exchange and correlation together provide the correct description of weak bonds and that the (dynamical) correlation part should be responsible for the dispersion binding [65]. We show that this is indeed the case for LAK by comparing the $Ar_2$ binding curve of LAK exchange with that of exact exchange in Fig. 2 of the Supplemental Material [45].

Figure 2(a) shows $F_{\text{x}}^{\text{SCAN}}$, $F_{\text{x}}^{\text{TASK}}$, and $F_{\text{x}}^{\text{LAK}}$ (all scaled by a factor of 10) along the bond axis $z$ of the argon dimer at the experimental equilibrium bond length 3.758 Å [66] (solid lines) and the argon atom (dotted lines). Each enhancement factor is obtained from a self-consistent all-electron calculation with the respective functional in the DARSEC code [67,68], a real-space code for diatomic molecules and atoms. Additionally, we show $r_s$ and the meta-GGA ingredients $s$ and $\alpha$, as obtained from the calculation with LAK. As discussed above, $\alpha$ becomes zero in single-orbital regions and thus at the position of the nucleus, whereas it becomes large in regions of density overlap between closed shells such as at the bond center of $Ar_2$ and in the asymptotic tail of the density far from the nucleus. The gradient of the density, and thus also $s$, vanishes at the bond center. Except for the binding region, $s$ and $\alpha$ are undistinguishable for the atom and the dimer. Therefore, the same holds for the enhancement factors.

Figure 2(b) shows the exchange enhancement factors $F_{\text{x}}^{\text{SCAN}}$, $F_{\text{x}}^{\text{TASK}}$, and $F_{\text{x}}^{\text{LAK}}$ as functions of $s$ for $\alpha = 0$, $\alpha = 1$, and $\alpha \to \infty$. All three enhancement factors share the same limit for $\alpha = 0$. Additionally, all three functionals share the same asymptotic decay as $s^{-1/2}$ for $s \to \infty$. Therefore, all three enhancement factors are very similar for the asymptotic tail of the density, especially LAK and TASK, compare the large z limit of Fig. 2(a). Because the enhancement factors of LAK and TASK therefore only show significant differences – both between each other and between atom and molecule – in the binding region, the decisively different binding behavior of LAK and TASK for rare gas dimers must be due to their different behavior in this region. Figure 2(c), therefore, shows a version of Fig. 2(a) zoomed in on the binding region.

Since the binding region is only present in the dimer, $s$ and $\alpha$ in this region differ decisively between the atom and dimer. In fact, starting from the nucleus, first $\alpha$ becomes different at $\alpha \approx 0.4$, rising much faster for the dimer due to the increased density overlap between the two atoms. Slightly closer to the center of the bond, also $s$ starts to differ. Starting from $s \approx 1.2$, the reduced density gradient of the atom increases faster than that of the dimer. In the latter, $s$ reaches a peak value of $s \approx 1.7$, begins to decrease and eventually becomes zero at the center of the bond. Thus, regions of $s \lesssim 1.2$ are more energetically relevant in the dimer, whereas regions of $s \gtrsim 1.2$ are more energetically relevant in the atom. This finding is in

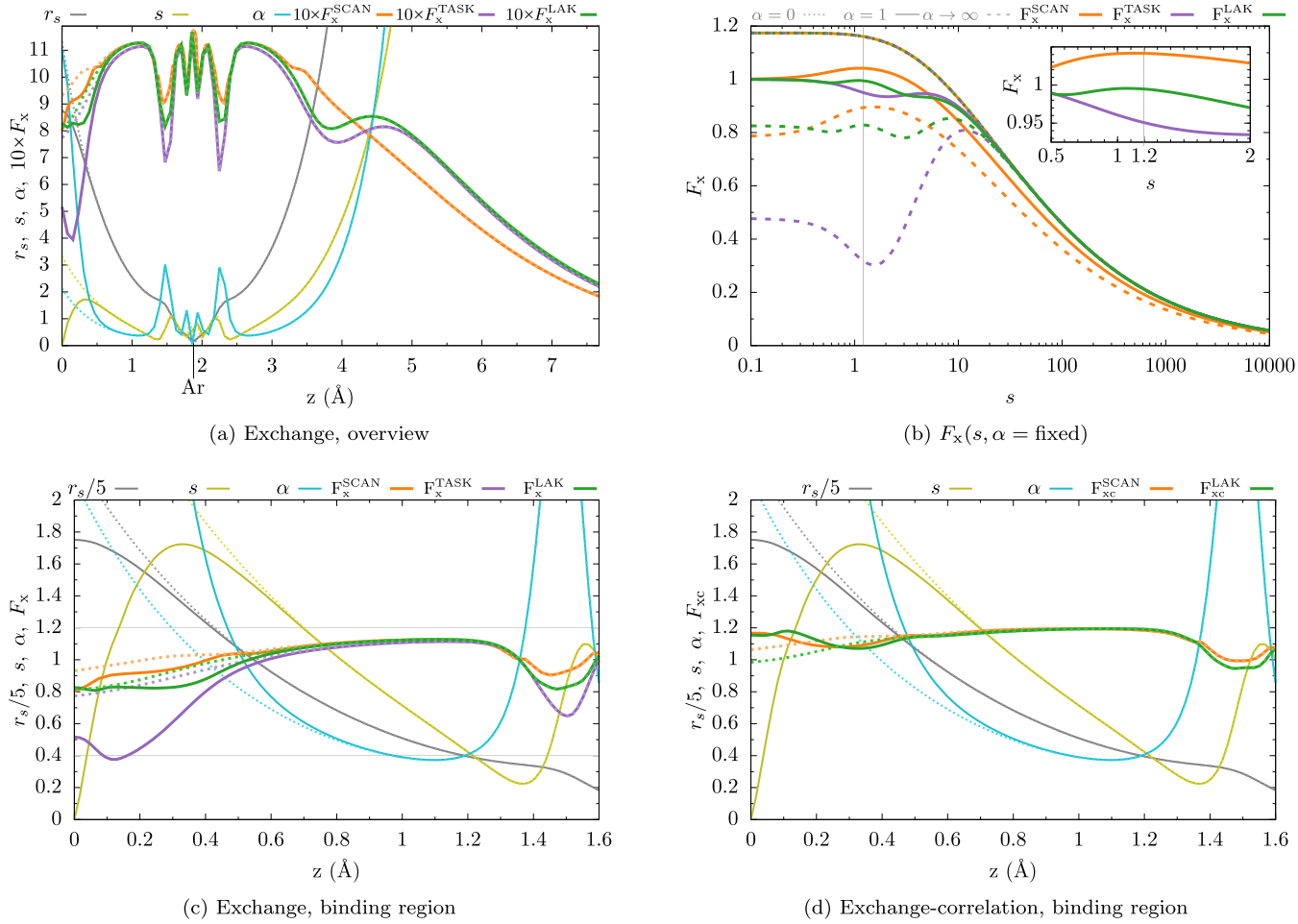


(a) Exchange, overview

(b) $F_x(s, \alpha = \text{fixed})$

(c) Exchange, binding region

(d) Exchange-correlation, binding region

FIG. 2. (a), (c), and (d): Enhancement factors of SCAN, TASK, and LAK along the bond axis $z$ of the argon dimer at equilibrium distance (solid lines) and for the argon atom (dotted lines). The position of the nuclei is $-1.879$ Å and 1.879 Å for the dimer and 1.879 Å for the atom. The horizontal gray lines in (c) mark $\alpha = 0.4$ and $s = 1.2$. (b) Exchange enhancement factors of SCAN, TASK, and LAK as functions of $s$ for $\alpha = 0$ (dotted), $\alpha = 1$ (solid), and $\alpha \to \infty$ (dashed). The vertical gray lines mark $s = 1.2$. Since all three exchange enhancement factors are equivalent for $\alpha = 0$, the lines for $\alpha = 0$ coincide.

line with the analysis of Jenkins and coworkers [62,63], which showed that in GGAs regions with $\partial F_x/\partial s > 0$ contribute attractively to the binding if $s \lesssim 1.2$ and repulsively if $s \gtrsim 1.2$. Consequently, semilocal density functionals predict a stronger binding of weakly interacting systems if they have a local maximum in $s$ near $s = 1.2$. Our results are further consistent with Ref. [13], where the authors pointed out that inflection points in the $s$ dependence of the enhancement factor are important for the description of weakly interacting systems. Ultimately, these insights have been the basis of the second construction principle of LAK [36].

Additionally, Fig. 2(c) clarifies the situation regarding the $\alpha$ dependence, as it suggests a similar criterion for $\alpha$: regions of $\partial F_x/\partial\alpha > 0$ contribute attractively to the exchange binding for $\alpha \gtrsim 0.4$. This can be seen as follows. Starting from the nucleus, $\alpha$ is equivalent in the monomer and the dimer until $\alpha$ starts to rise faster in the dimer at about 1 Å from the bond center. However, between 1 Å and 0.4 Å from the bond center, the electron density, i.e., $r_s$, is almost the same in the monomer and the dimer. Consequently, in the dimer $\alpha$ is larger than in the monomer at equivalent local densities. A similar argument holds for regions closer than 0.4 Å to the bond center. Thus, the dimer is favored energetically if $F_x$ rises in $\alpha$ for $\alpha \gtrsim 0.4$. This implies the criterion $\partial F_x/\partial\alpha > 0$ for $\alpha \gtrsim 0.4$ for increased van der Waals binding [69]. It is questionable if the $\alpha$ dependence for $\alpha \lesssim 0.4$ plays any role at all for the binding because, except for the core region, $\alpha$ rarely becomes smaller than 0.4 in both the argon atom and dimer. To validate the latter, an analysis along the lines of Refs. [62,63] focusing on $\alpha$ would be a worthwhile task for future research.

Inspection of Fig. 2(b) shows that $F_x^{LAK}$ has a local maximum at $s = 1.2$ for the relevant values of $\alpha > 0.4$, while $F_x^{SCAN}$ has a local maximum and $F_x^{TASK}$ a local minimum at slightly larger reduced density gradients. While the local maxima of SCAN and LAK are attractive, the local minimum of TASK is repulsive. Additionally, all three enhancement factors decrease with $\alpha$ [36,70] and this decrease is much more pronounced in LAK and TASK than in SCAN (this essentially reflects the construction principle of TASK and construction principle one of LAK). Thus, the $\alpha$ dependence of all three functionals contributes repulsively. Especially for $\alpha > 1$, $\partial F_x/\partial\alpha$ of TASK is clearly the most negative, as can be seen by comparing SCAN, TASK, and LAK for $\alpha = 1$ and $\alpha \to \infty$ in Fig. 2(b). As a result, TASK acts extremely

repulsively since both its $s$ and its $\alpha$ dependence are strongly repulsive and $F_x^{\mathrm{TASK}}$ is, therefore, significantly smaller in the dimer around the center of the bond. Consequently, TASK penalizes the bond energetically and avoids the accumulation of density between the two closed-shell systems.

SCAN and LAK have a more balanced binding behavior. This is reflected in Fig. 2(c) in the fact that $F_x^{\mathrm{TASK}}$ is much smaller in the dimer near the bond center of the dimer than in the corresponding distance from the nucleus of the single atom, whereas there is almost no difference for $F_x^{\mathrm{SCAN}}$ and only a small difference for $F_x^{\mathrm{LAK}}$. Although this makes LAK exchange and SCAN exchange significantly less repulsive than TASK exchange, neither just by itself predicts binding at the equilibrium distance, as seen in Fig. 2 of the Supplemental Material [45]. Instead, only the inclusion of the correlation parts in LAK and SCAN leads to the appropriate binding.

Therefore, we now extend the analysis to exchange and correlation together in Fig. 2(d). For exchange and correlation together, the differences between SCAN and LAK are much smaller than for their exchange parts alone. This is because, on the one hand, SCAN is constructed such that all its derivatives with respect to $\alpha$ vanish at $\alpha = 1$, giving rise to small kinks in $F_x^{\mathrm{SCAN}}(z)$ and $F_{xc}^{\mathrm{SCAN}}(z)$ whenever $\alpha = 1$. LAK correlation, on the other hand, counteracts the $\alpha$ dependence of exchange (a condition required for the expected signs of the exchange and correlation contributions to the derivative discontinuity [60]), and therefore, increases the binding of the argon dimer.

Our results regarding the $s$ dependence might seem to be in conflict with earlier studies that argue that for GGAs the large-gradient behavior of exchange would be decisive for the description of weakly interacting systems [3,10,14,47,61,71]. However, our results are in line with other studies [7,31] that attributed the above-mentioned finding to the fact that the small-gradient behavior of GGAs is typically determined by the gradient expansion and therefore usually very similar. Thus, the description of *weak* interactions in GGAs can be modified by their behavior for large $s$. Meta-GGAs, on the other hand, provide an additional degree of freedom in the gradient expansion, allowing a much greater variety of small s behaviors to be compatible with the gradient expansion [36]. Therefore, the actually dominant influence of $s$ around 1.2 [62,63] becomes more important in meta-GGAs.

In summary, our analyses for the argon dimer confirm the findings of Refs. [13,62,63]: Local maxima and inflection points in the $s$ dependence of the enhancement factor are decisive for correctly describing weakly interacting systems with semilocal DFT. More precisely, $\partial F_{xc}/\partial s > 0$ increases the binding if $s \lesssim 1.2$ and decreases the binding if $s \gtrsim 1.2$. Furthermore, our analyses suggest a similar criterion for $\alpha$: $\partial F_{xc}/\partial \alpha < 0$ for $\alpha \gtrsim 0.4$ decreases the binding of weakly interacting systems.

## IV. LAK FOR GENERAL THERMOCHEMISTRY

We are aware that good results for the rare gas binding curves do not guarantee good results for dispersion interactions, in general, in particular for organic and biological systems [31]. Moreover, good results for dispersion interactions alone are not sufficient in typical applications, but the accurate description of both, noncovalent and covalent interactions is important. To this end, we test LAK on the large general main-group thermochemistry, kinetics, and noncovalent interactions (GMTKN55) database [37].

The GMTKN55 database includes basic properties and reaction energies of small molecules, reaction energies for large systems and isomerization reactions, barrier heights, and inter- and intramolecular noncovalent interactions. To make these different quantities comparable, density functionals are typically benchmarked on GMTKN55 using the weighted total mean absolute deviation WTMAD-2 [72]. Table I summarizes the WTMAD-2 of several nonempirical semilocal density functionals, including LAK and the best-performing dispersion-corrected semilocal density functionals for the GMTKN55 database and its subcategories. We did not include TASK in Table I because TASK is not particularly well suited for the description of energetic bonds [40,73], and as explained above, noncovalent interactions (WTMAD-2 of 48.24 kcal/mol). The results for the pure density functionals, i.e., density functionals without additional dispersion correction, were obtained from fully self-consistent all-electron calculations in ADF [57,58]. We use the QZ4P basis set except for the anions in the GMKTN55 database, which require more diffuse basis functions. Therefore, we use the AUG/ATZ2P augmented basis set for all anions. We ensure benchmarking accuracy by using EXCELLENT numerical accuracy and a RADIALGRIDBOOST of 3. Our results for PBE and SCAN are in line with those of Ref. [37], given that a different code is used. The results for the dispersion corrected methods are from the literature. The detailed data for all subsets are provided in the Supplemental Material [45].

Table I reveals a central result of this work. It shows that LAK is, to the best of our knowledge, the best-performing pure semilocal density functional on the GMTKN55 database. In Ref. [37] from 2017, a large number of density functionals were tested on GMTKN55, and the best-performing semilocal density functionals were M06-L (WTMAD-2 of 8.67 kcal/mol) and SCAN (8.72 kcal/mol). To the best of our knowledge, r2SCAN with a WTMAD-2 of 8.49 kcal/mol is the only semilocal density functional that has been able to surpass this value since then. LAK improves this with a WTMAD-2 of 7.77 kcal/mol.

Taking a look at the subcategories of GMTKN55 in Fig. 3 reveals that LAK achieves this improvement by matching the accuracy of r2SCAN for the covalent interactions of small and large molecules, while improving upon r2SCAN for barrier heights and noncovalent interactions.

LAK reaches an accuracy that is comparable even to the best dispersion-corrected semilocal density functionals for GMTKN55, and is more accurate than all dispersion-corrected semilocal density functionals reported in Ref. [37]. Only SCAN-D3 with an WTMAD-2 of 7.86 kcal/mol reaches a similar accuracy as LAK. Since 2017, only r2SCAN-D4 [74] with a WTMAD-2 of 7.54 kcal/mol, and the semi-empirical B97M-V [34] with a WTMAD-2 of 5.46 kcal/mol [75] (and their respective r2SCAN+rVV10 [76], r2SCAN-3c [77], B97M-D3, and B97M-D4 [78] variants) improved upon SCAN-D3. Figure 4 compares LAK with the best-performing dispersion-corrected semilocal methods B97M-V and r2SCAN-D4. While LAK and r2SCAN-D4 are on par for the WTMAD-2 database as a whole, their performance

TABLE I. WTMAD-2 in kcal/mol for the GMTKN55 database [37] and its subcategories. Upper half of the table: Nonempirical semilocal density functionals; data from this work. Lower half of the table: Semilocal density functionals with dispersion correction optimized for (parts of) GMTKN55; data from the literature. The Supplemental Material [45] reports the error statistics for the subsets of GMTKN55.

| | Basic | Large | BHs | Intermol. NCIs | Intramol. NCIs | All NCIs | GMTKN55 |
|---|---|---|---|---|---|---|---|
| PBE | 6.82 | 15.99 | 16.69 | 15.62 | 19.46 | 17.50 | 13.79 |
| SCAN | 5.28 | 8.76 | 14.88 | 10.24 | 8.20 | 9.24 | 8.65 |
| r2SCAN | 4.98 | 9.04 | 13.80 | 10.49 | 8.10 | 9.32 | 8.49 |
| LAK | 5.12 | 8.83 | 11.42 | 9.49 | 6.95 | 8.25 | 7.77 |
| SCAN-D3 [37] | 5.31 | 7.86 | 14.94 | 8.50 | 6.61 | 7.58 | 7.86 |
| r2SCAN-D4 [74] | 5.55 | 8.26 | 14.29 | 7.46 | 5.74 | 6.62 | 7.54 |
| B97M-V [75] | 3.68 | 9.30 | 7.52 | 3.56 | 5.76 | 4.64 | 5.46 |

for the subcategories differs. While LAK is more accurate for the barrier heights, r2SCAN-D4 is more accurate for the noncovalent interactions. The latter finding is expected, as the parameters of the D4 dispersion correction of r2SCAN-D4 are fitted to subsets of GMTKN55 for noncovalent interactions, whereas LAK is a nonempirical pure density functional.

B97M-V shows a significant improvement over LAK and r2SCAN-D4 for all quantities except for the reaction energies and for the intramolecular noncovalent interactions of r2SCAN-D4. Given that B97M-V is constructed semiempirically based on parts of the GMTKN55 database, this is not too surprising. Nevertheless, the amount of improvement indicates that the additional flexibility of the combined approach of B97M-V, namely, designing the semilocal density functional together with a dispersion correction [33,34], can yield improved results for thermochemistry and kinetics. A nonempirical meta-GGA based on a partitioning of the gradient expansion similar to LAK, but designed together with a dispersion correction, and consequently most likely dropping the second construction principle of LAK, thus represents an interesting target for future research.

It is worth looking at two specific subsets of the GMTKN55. The major shortcoming of semilocal density functionals is their fundamental inability to fully cancel the Hartree self-energy. This can be seen from the SIE4×4 set of self-interaction error-related problems, for which LAK has a mean absolute deviation (MAD) of 17.29 kcal/mol, r2SCAN of 17.90 kcal/mol, and M06-L of 17.94 kcal/mol. This indicates that LAK improves only marginally upon other popular meta-GGAs for self-interaction problems. Another noteworthy subset is the MB16-43 set of decomposition energies of artificial molecules [79]. Due to its "mindless" design, it can serve as an indicator of the transferability of a density functional to novel chemistry [80]. It is often reported that nonempirical density functionals are more transferable than empirical ones, and their respective performance on MB16-43 supports this view [74,77]: While the MADs of the empirical M06-L (64.05 kcal/mol) and the semi-empirical B97M-V (35.35 kcal/mol [75]) are high, the nonempirical

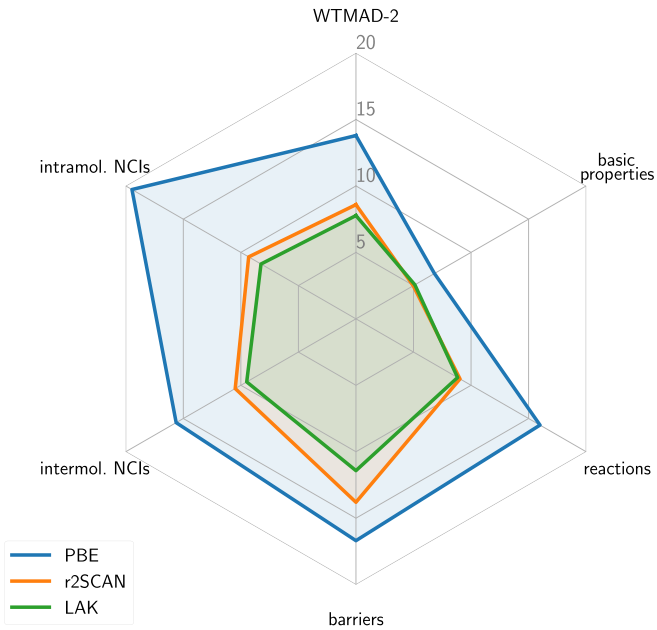


FIG. 3. WTMAD-2 in kcal/mol for the GMTKN55 database and its subcategories for selected nonempirical semilocal density functionals: the GGA PBE, the meta-GGA r2SCAN, and the meta-GGA LAK.

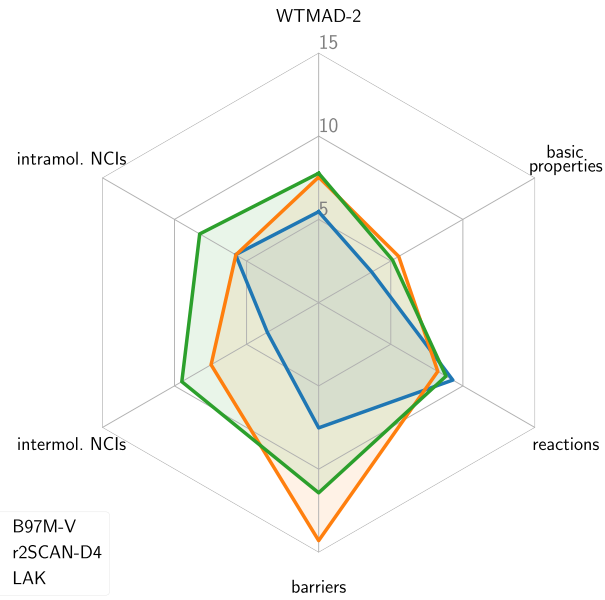


FIG. 4. WTMAD-2 in kcal/mol for the GMTKN55 database and its subcategories: LAK compared with the best-performing dispersion-corrected semilocal functionals B97M-V and r2SCAN-D4.

functionals PBE (23.34 kcal/mol), SCAN (15.74 kcal/mol), and r2SCAN (12.83 kcal/mol) are systematically and significantly more accurate for MB16-43. LAK has a MAD of 16.36 kcal/mol on MB16-43, similar to the MAD of SCAN, emphasizing its nonempirical nature and suggesting a similar transferability to novel chemistry as SCAN. It is worth to mention that compared to other semilocal-cost functionals, LAK has the additional advantage of considerably improving the prediction of band gaps, as detailed in Ref. [36].

## V. ENHANCEMENT FACTOR ENGINEERING: DENSITY FUNCTIONALS BASED ON INSIGHTS FROM MATHEMATICS, PHYSICS, AND CHEMISTRY

In the construction of LAK [36], we extend the successful design strategy for nonempirical density functionals (e.g., Refs. [38–40,81–84]) of combining exact constraints with exactness for model systems, so-called appropriate norms, by the further nonempirical concept of construction principles. In the following we explain the idea behind this strategy of designing exchange-correlation functionals.

A semilocal exchange-correlation functional, and thus the approximation to all electron-electron interactions, is completely defined by its enhancement factor. On the one hand, the exact constraints and model systems restrict the enhancement factor through inequalities, scaling relations, and exact limits [84]. On the other hand, the degree of nonlocality of a density funcitonal depends to a large extent on the details of its enhancement factor in between these limits. However, the exact constraints and model systems provide only limited information on how the enhancement factor should be modeled in this intermediate range. Therefore, the construction principles guide the enhancement factor in the intermediate range to ensure proper nonlocality. In the case of LAK, these are the ultranonlocality associated with the derivative discontinuity and the short- and intermediate-range van der Waals interactions.

Importantly, we consider the *graph* of the enhancement factor the decisive property that should be obtained in a nonempirical fashion. The graph defines the enhancement factor and thus the density functional uniquely. Experience has shown that a lot of information about the performance of a functional can be obtained just from the graph [70]. Furthermore, all exact constraints, appropriate norms, and construction principles also apply to the graph. In addition, we aim for a smooth enhancement factor, a condition found to be important for more accurate densities and the numerically stability of density functional approximations [85]. Given these conditions, it is then up to us to find a suitable representation of the graph in terms of functions. While Occam's razor advises us to find the simplest possible representation of the graph, it remains a mathematical problem to find functions that can generate this graph.

Following the argumentation above, the construction principles thus guide the graph of the enhancement factor in a range in which the graph was not previously determined by physical reasons. In other words, the construction principles are additional conditions that tailor the choice of mathematical functions that satisfy the exact constraints and appropriate norms, based on chemical and physical insights. Because we design our functional via conditions on the graph of its enhancement factor, we call this design strategy "enhancement factor engineering."

Notably, using a *limited* number of parameters to represent the graph can make it easier to find a suitable representation of the graph in terms of functions. We want to emphasize that the parameters introduced in this way are only a means to the end of representing the graph, and are therefore fundamentally different from parameters determined, e.g., by fitting to databases. Moreover, the use of too many parameters is prevented by the condition of a smooth enhancement factor. At this point, we want to emphasize that parameters in a method are not empirical per se, but that it depends on how they are fixed. If they are fixed by fitting to databases, they are empirical. In contrast, if they are fixed by mathematical constraints, we regard them as nonempirical. However, for a given enhancement factor, one can always find more general functions from which one can obtain this enhancement factor by fixing several parameters (e.g., quasitrivially by setting them to zero or one) [86]. The *graph* of the enhancement factor, however, is independent of its parametrization and thus of any parameters.

The motivation for the design strategy of enhancement factor engineering emerges from the following considerations. From a mathematical point of view, we desire the enhancement factor to satisfy as many analytical conditions as possible that we know from the exact exchange-correlation functional. This is achieved by adhering to the exact constraints. From a physical point of view, we additionally want the enhancement factor to be correct for certain model systems, such as the homogeneous electron gas. These are the appropriate norms. Finally, from a chemical point of view, we wish to include existing chemical intuition into the enhancement factor. From the authors' point of view, taking into account existing knowledge about electronic structure or chemical intuition does not mean fitting parameters to large databases, but rather incorporating known facts about the electronic structure of certain types of systems into the design of the graph of the enhancement factor. This leads to the construction principles. In this sense, the strategy of enhancement factor engineering combines the insights from mathematics, physics, and chemistry.

## VI. WHEN TO CHOOSE THE LAK EXCHANGE-CORRELATION FUNCTIONAL

The zoo of density functionals is constantly growing and it is often hard to choose an appropriate functional for a given task. Therefore, we provide our current view of the advantages and disadvantages of LAK, and highlight areas where LAK could be an attractive choice.

Figure 5 summarizes the performance of LAK reported in Ref. [36], complemented by the performance of LAK for the S22 set of weak interactions [87,88]. As in Sec. II, we compare LAK with PBE, SCAN, and M06-L. However, due to its inadequacy with respect to weak interactions, we replace TASK with the range-separated hybrid HSE06 [89,90], which has become the de-facto standard for DFT band structure prediction, and is, therefore, often used in materials

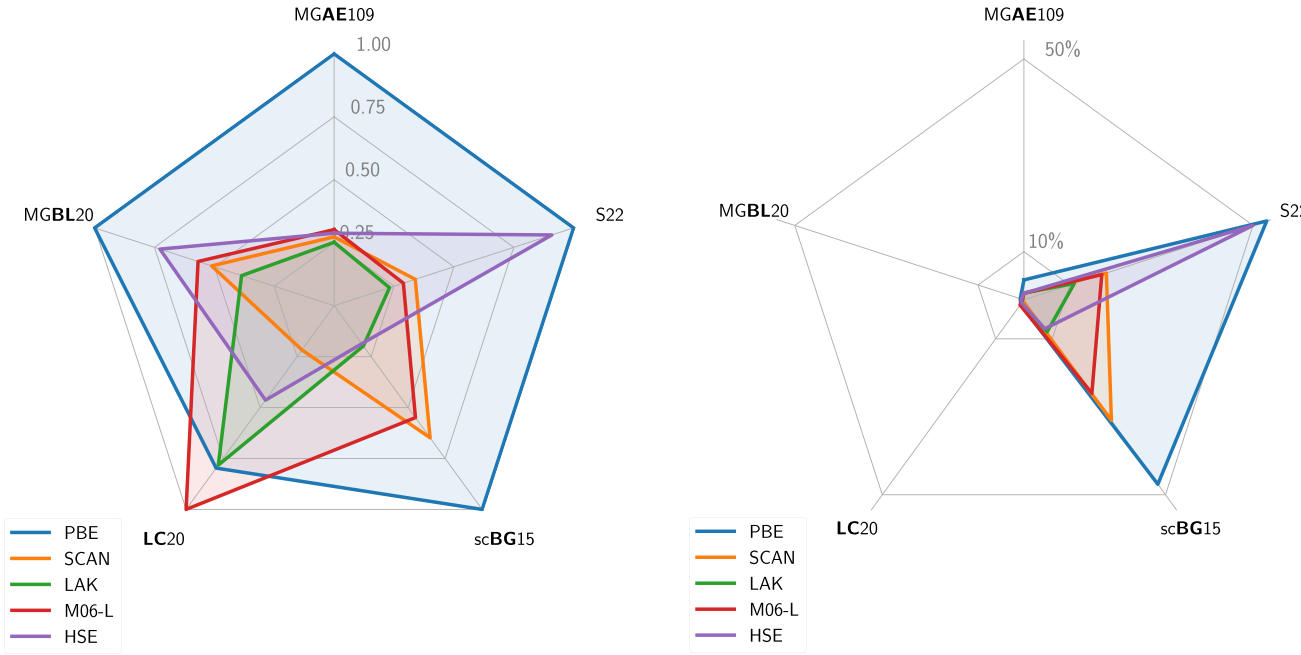


FIG. 5. General performance of selected density functionals for main-group atomization energies (MGAE109) [91], main-group bond lengths (MGBL20) [92], lattice constants (LC20) [93], semi-conductor band gaps (scBG15) [36], and weak interactions (S22) [87,88]. Left: MAD relative to the worst performing functional for each category. Right: Mean absolute relative deviation from the reference values.

simulations. The left-hand side shows the mean absolute deviation relative to the worst performing density functional in the respective category. LAK performs best or almost best for all properties except for the lattice constants. To estimate the importance of LAK's attractive accuracy for band gaps, covalent and weak interactions against its relatively less accurate lattice constants, we compare the mean absolute *relative* deviation from the reference values on the right-hand side of Fig. 5. While the relative error in the lattice constants is below 2% for all tested functionals, LAK is the only functional that achieves relative errors of about 10% for band gaps and weak interactions. Although highly accurate lattice constants are critical in some applications, the broad spectrum of properties that LAK can accurately predict makes it an attractive choice for large-scale materials simulations that require high accuracy for a large variety of properties at low computational cost.

Another important aspect for practical calculations, especially for high-throughput calculations, is numerical stability [94]. Therefore, this paragraph discusses the numerical stability and numerical convergence of LAK. Remarkably, both LAK and TASK did not show any convergence issues for any of the 2462 single-point calculations of the GMTKN55 database. The numerical stability of LAK and TASK is supported by recent findings [36,59,73,95,96]. To assess the numerical convergence, Figure 6 shows the mean absolute error for the S22 set of weak interactions with respect to the number of grid points. We compare LAK with M06-L, SCAN, and r2SCAN, because M06-L and SCAN are well known for their accuracy for weakly interacting systems and r2SCAN is a revised version of SCAN with improved numerical stability and numerical convergence [82]. While SCAN, and to a lesser extend M06-L, exhibit well-reported numerical convergence issues [52,59], LAK and r2SCAN are already fully converged with ADF's BECKEGRID NUMERICALACCURACY NORMAL. Of course, the situation might be different for other types of systems.

In the following, we highlight several areas where we consider LAK a possible improvement over existing density functionals by providing either higher accuracy at similar computational cost, or similar accuracy at strongly reduced computational cost. We write this at a time when LAK has not yet been tested extensively, i.e., the following statements are to be seen as "hopefully educated guesses." Its balanced accuracy for band gaps and energetic binding together with its reasonable description of noncovalent interactions makes

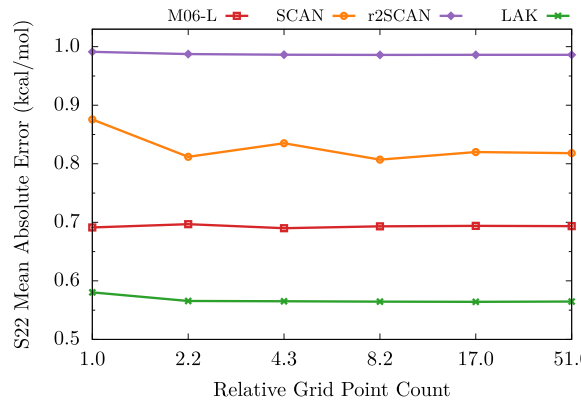


FIG. 6. Mean absolute error (MAE) of interaction energies of weakly interacting complexes (kcal/mol) for the S22 set [87,88] as a function of increasing numerical integration grid density expressed relative to the smallest grid. The grids are chosen via the BECKEGRID NUMERICALACCURACY keyword in ADF from left to right: BASIC, NORMAL, GOOD, VERYGOOD, and EXCELLENT all with a fixed RADIALGRIDBOOST of 1. For the highest accuracy, we use BECKEGRID NUMERICALACCURACY EXCELLENT with a RADIALGRIDBOOST of 3.

LAK a promising functional for surface and interface problems, as well as biological systems in which covalent and weak interactions play together. Last but not least, LAK (and equally well TASK for this task) can predict the band structure of semiconductors with a similar quality as HSE, but at a fraction of HSE's computational cost [60].

## ACKNOWLEDGMENTS

The authors thank J. Sun for helpful discussions on the rare gas dimers. We appreciate financial support from the Deutsche Forschungsgemeinschaft, DFG Project No. 457582427, from the Bavarian State Ministry of Science, Research, and the Arts for the Collaborative Research Network "Solar Technologies go Hybrid," and from the Elite Study Program "Biological Physics" of the Elite Network of Bavaria.

T.L. and S.K. conceptualized the work. T.L. performed the research, wrote the required routines, ran the calculations, and analyzed the results. T.L. wrote the first draft of the manuscript. T.L. and S.K. worked out the final manuscript.

The LAK meta-GGA is available in AMS, in particular in ADF and BAND (in the trunk and since AMS2025), as well as in VASP (since version 6.5.0).

[1] A. J. Cohen, P. Mori-Sánchez, and W. Yang, Challenges for density functional theory, Chem. Rev. **112**, 289 (2012).

[2] B. I. Lundqvist, Y. Andersson, H. Shao, S. Chan, and D. C. Langreth, Density functional theory including van der Waals forces, Int. J. Quantum Chem. **56**, 247 (1995).

[3] Y. Zhang, W. Pan, and W. Yang, Describing van der Waals Interaction in diatomic molecules with generalized gradient approximations: The role of the exchange functional, J. Chem. Phys. **107**, 7921 (1997).

[4] W. Kohn, Y. Meir, and D. E. Makarov, Van der Waals energies in density functional theory, Phys. Rev. Lett. **80**, 4153 (1998).

[5] M. Lein, J. F. Dobson, and E. K. U. Gross, Toward the description of van der Waals interactions within density functional theory, J. Comput. Chem. **20**, 12 (1999).

[6] T. Van Mourik and R. J. Gdanitz, A critical note on density functional theory studies on rare-gas dimers, J. Chem. Phys. **116**, 9620 (2002).

[7] J. Tao and J. P. Perdew, Test of a nonempirical density functional: Short-range part of the van der Waals interaction in rare-gas dimers, J. Chem. Phys. **122**, 114102 (2005).

[8] I. C. Gerber and J. G. Ángyán, London dispersion forces by range-separated hybrid density functional with second order perturbational corrections: The case of rare gas complexes, J. Chem. Phys. **126**, 044103 (2007).

[9] K. Pernal, R. Podeszwa, K. Patkowski, and K. Szalewicz, Dispersionless density functional theory, Phys. Rev. Lett. **103**, 263201 (2009).

[10] F. O. Kannemann and A. D. Becke, Van der Waals interactions in density-functional theory: Rare-gas diatomics, J. Chem. Theory Comput. **5**, 719 (2009).

[11] J. P. Perdew, J. Sun, R. M. Martin, and B. Delley, Semilocal density functionals and constraint satisfaction, Int. J. Quantum Chem. **116**, 847 (2016).

[12] H. Peng, Z.-H. Yang, J. P. Perdew, and J. Sun, Versatile van der Waals density functional based on a meta-generalized gradient approximation, Phys. Rev. X **6**, 041005 (2016).

[13] J. H. Yang, D. A. Kitchaev, and G. Ceder, Rationalizing accurate structure prediction in the meta-GGA SCAN functional, Phys. Rev. B **100**, 035132 (2019).

[14] A. J. A. Price, K. R. Bryenton, and E. R. Johnson, Requirements for an accurate dispersion-corrected density functional, J. Chem. Phys. **154**, 230902 (2021).

[15] K. R. Bryenton, A. A. Adeleke, S. G. Dale, and E. R. Johnson, Delocalization error: The greatest outstanding challenge in density-functional theory, WIREs Comput. Mol. Sci. **13**, e1631 (2023).

[16] M. Dion, H. Rydberg, E. Schröder, D. C. Langreth, and B. I. Lundqvist, Van der Waals density functional for general geometries, Phys. Rev. Lett. **92**, 246401 (2004) [**95**, 109902(E) (2005)].

[17] O. A. Vydrov and T. Van Voorhis, Nonlocal van der Waals density functional: The simpler the better, J. Chem. Phys. **133**, 244103 (2010).

[18] R. Sabatini, T. Gorni, and S. de Gironcoli, Nonlocal van der Waals density functional made simple and efficient, Phys. Rev. B **87**, 041108(R) (2013).

[19] S. Grimme, Accurate description of van der Waals complexes by density functional theory including empirical corrections, J. Comput. Chem. **25**, 1463 (2004).

[20] A. D. Becke and E. R. Johnson, A density-functional model of the dispersion interaction, J. Chem. Phys. **123**, 154101 (2005).

[21] A. Tkatchenko and M. Scheffler, Accurate molecular Van der Waals interactions from ground-state electron density and free-atom reference data, Phys. Rev. Lett. **102**, 073005 (2009).

[22] S. Grimme, Density functional theory with london dispersion corrections, WIREs Comput. Mol. Sci. **1**, 211 (2011).

[23] S. Grimme, A. Hansen, J. G. Brandenburg, and C. Bannwarth, Dispersion-corrected mean-field electronic structure methods, Chem. Rev. **116**, 5105 (2016).

[24] H. Eshuis and F. Furche, A parameter-free density functional that works for noncovalent interactions, J. Phys. Chem. Lett. **2**, 983 (2011).

[25] E. Trushin, A. Thierbach, and A. Görling, Toward chemical accuracy at low computational cost: Density-functional theory with $\sigma$-functionals for the correlation energy, J. Chem. Phys. **154**, 014104 (2021).

[26] Y. Zhao and D. G. Truhlar, A new local density functional for main-group thermochemistry, transition metal bonding, thermochemical kinetics, and noncovalent interactions, J. Chem. Phys. **125**, 194101 (2006).

[27] G. K. H. Madsen, L. Ferrighi, and B. Hammer, Treatment of layered structures using a semilocal meta-GGA density functional, J. Phys. Chem. Lett. **1**, 515 (2010).

[28] J. Sun, B. Xiao, Y. Fang, R. Haunschild, P. Hao, A. Ruzsinszky, G. I. Csonka, G. E. Scuseria, and J. P. Perdew, Density functionals that recognize covalent, metallic, and weak bonds, Phys. Rev. Lett. **111**, 106401 (2013).

[29] J. Sun, R. C. Remsing, Y. Zhang, Z. Sun, A. Ruzsinszky, H. Peng, Z. Yang, A. Paul, U. Waghmare, X. Wu *et al.*, Accurate first-principles structures and energies of diversely bonded systems from an efficient density functional, Nat. Chem. **8**, 831 (2016).

[30] M. J. Allen and D. J. Tozer, Eigenvalues, integer discontinuities and nmr shielding constants in Kohn-Sham theory, Mol. Phys. **100**, 433 (2002).

[31] A. Ruzsinszky, J. P. Perdew, and G. I. Csonka, Binding energy curves from nonempirical density functionals II. van der Waals bonds in rare-gas and alkaline-earth diatomics, J. Phys. Chem. A **109**, 11015 (2005).

[32] A. Patra, J. E. Bates, J. Sun, and J. P. Perdew, Properties of real metallic surfaces: Effects of density functional semilocality and van der Waals nonlocality, Proc. Natl. Acad. Sci. USA **114**, E9188 (2017).

[33] S. Grimme, Semiempirical GGA-type density functional constructed with a long-range dispersion correction, J. Comput. Chem. **27**, 1787 (2006).

[34] N. Mardirossian and M. Head-Gordon, Mapping the genome of meta-generalized gradient approximation density functionals: The search for B97M-V, J. Chem. Phys. **142**, 074111 (2015).

[35] N. Mardirossian and M. Head-Gordon, $\omega$B97M-V: A combinatorially optimized, range-separated hybrid, meta-GGA density functional with VV10 nonlocal correlation, J. Chem. Phys. **144**, 214110 (2016).

[36] T. Lebeda, T. Aschebrock, and S. Kümmel, Balancing the contributions to the gradient expansion: Accurate binding and band gaps with a nonempirical Meta-GGA, Phys. Rev. Lett. **133**, 136402 (2024).

[37] L. Goerigk, A. Hansen, C. Bauer, S. Ehrlich, A. Najibi, and S. Grimme, A look at the density functional theory zoo with the advanced GMTKN55 database for general main group thermochemistry, kinetics and noncovalent interactions, Phys. Chem. Chem. Phys. **19**, 32184 (2017).

[38] J. P. Perdew, K. Burke, and M. Ernzerhof, Generalized gradient approximation made simple, Phys. Rev. Lett. **77**, 3865 (1996).

[39] J. Sun, A. Ruzsinszky, and J. P. Perdew, Strongly constrained and appropriately normed semilocal density functional, Phys. Rev. Lett. **115**, 036402 (2015).

[40] T. Aschebrock and S. Kümmel, Ultranonlocality and accurate band gaps from a meta-generalized gradient approximation, Phys. Rev. Res. **1**, 033082 (2019).

[41] R. Hellmann, E. Bich, and E. Vogel, *Ab initio* potential energy curve for the neon atom pair and thermophysical properties of the dilute neon gas. I. Neon–neon interatomic potential and rovibrational spectra, Mol. Phys. **106**, 133 (2008).

[42] B. Jäger, R. Hellmann, E. Bich, and E. Vogel, *Ab initio* pair potential energy curve for the argon atom pair and thermophysical properties of the dilute argon gas. I. Argon–argon interatomic potential and rovibrational spectra, Mol. Phys. **107**, 2181 (2009).

[43] B. Jäger, R. Hellmann, E. Bich, and E. Vogel, State-of-the-art *ab initio* potential energy curve for the krypton atom pair and thermophysical properties of dilute krypton gas, J. Chem. Phys. **144**, 114304 (2016).

[44] R. Hellmann, B. Jäger, and E. Bich, State-of-the-art *ab initio* potential energy curve for the xenon atom pair and related spectroscopic and thermophysical properties, J. Chem. Phys. **147**, 034304 (2017).

[45] See Supplemental Material at http://link.aps.org/supplemental/10.1103/PhysRevB.111.155133 for the detailed results for the subsets of the GMTKN55 database, the binding curve of He2, and the binding curve of Ar2 for exchange-only functionals.

[46] J. B. Anderson, An exact quantum Monte Carlo calculation of the helium–helium intermolecular potential. II, J. Chem. Phys. **115**, 4546 (2001) [**120**, 9886 (2004)].

[47] D. J. Lacks and R. G. Gordon, Pair interactions of rare-gas atoms as a test of exchange-energy-density functionals in regions of large density gradients, Phys. Rev. A **47**, 4681 (1993).

[48] D. C. Patton and M. R. Pederson, Application of the generalized-gradient approximation to rare-gas dimers, Phys. Rev. A **56**, R2495 (1997) [**71**, 019906(E) (2005)].

[49] D. C. Patton and M. R. Pederson, A theoretical study of rare-gas diatomic molecules with the generalized-gradient approximation to density functional theory, Int. J. Quantum Chem. **69**, 619 (1998).

[50] E. R. Johnson, R. A. Wolkow, and G. A. DiLabio, Application of 25 density functionals to dispersion-bound homomolecular dimers, Chem. Phys. Lett. **394**, 334 (2004).

[51] Y. Zhao and D. G. Truhlar, Comparative assessment of density functional methods for 3d transition-metal chemistry, J. Chem. Phys. **124**, 224105 (2006).

[52] E. R. Johnson, A. D. Becke, C. D. Sherrill, and G. A. DiLabio, Oscillations in meta-generalized-gradient approximation potential energy surfaces for dispersion-bound complexes, J. Chem. Phys. **131**, 034111 (2009).

[53] K. E. Yousaf and E. N. Brothers, Applications of screened hybrid density functionals with empirical dispersion corrections to rare gas dimers and solids, J. Chem. Theory Comput. **6**, 864 (2010).

[54] F. Tran and J. Hutter, Nonlocal van der Waals functionals: The case of rare-gas dimers and solids, J. Chem. Phys. **138**, 204103 (2013).

[55] L. Goerigk, Treating London-dispersion effects with the latest Minnesota density functionals: problems and possible solutions, J. Phys. Chem. Lett. **6**, 3891 (2015).

[56] J. P. Perdew and Y. Wang, Accurate and simple analytic representation of the electron-gas correlation energy, Phys. Rev. B **45**, 13244 (1992).

[57] SCM, Theoretical Chemistry, Vrije Universiteit, Amsterdam, The Netherlands, ADF 2023.104 (a modified version is used) (2023).

[58] G. te Velde, F. M. Bickelhaupt, E. J. Baerends, C. Fonseca Guerra, S. J. A. van Gisbergen, J. G. Snijders, and T. Ziegler, Chemistry with ADF, J. Comput. Chem. **22**, 931 (2001).

[59] S. Lehtola and M. A. L. Marques, Many recent density functionals are numerically ill-behaved, J. Chem. Phys. **157**, 174114 (2022).

[60] T. Lebeda, T. Aschebrock, J. Sun, L. Leppert, and S. Kümmel, Right band gaps for the right reason at low computational cost with a meta-GGA, Phys. Rev. Mater. **7**, 093803 (2023).

[61] É. D. Murray, K. Lee, and D. C. Langreth, Investigation of exchange energy density functional accuracy for interacting molecules, J. Chem. Theory Comput. **5**, 2754 (2009).

[62] T. Jenkins, K. Berland, and T. Thonhauser, Reduced-gradient analysis of van der Waals complexes, Electron. Struct. **3**, 034009 (2021).

[63] T. Jenkins, D. Chakraborty, K. Berland, and T. Thonhauser, Reduced-gradient analysis of molecular adsorption on graphene with nonlocal density functionals, Phys. Rev. B **109**, 035427 (2024).

[64] An earlier study on the influence of the $\alpha$ dependence on the description of weakly interacting systems reported findings that are not fully conclusive [28]: While the authors rationalize why a monotonically decreasing dependence on $\alpha$ could explain the increased binding of weakly interacting systems for one density functional, they note in the supplementary material that another functional with stronger decrease in $\alpha$ predicts less binding.

[65] M. D. Strømsheim, N. Kumar, S. Coriani, E. Sagvolden, A. M. Teale, and T. Helgaker, Dispersion interactions in density-functional theory: An adiabatic-connection analysis, J. Chem. Phys. **135**, 194109 (2011).

[66] *NIST Computational Chemistry Comparison and Benchmark Database*, edited by R. D. Johnson III, Available online: (accessed on November 1 2024) (NIST Standard Reference Database Number 101, 2022).

[67] A. Makmal, S. Kümmel, and L. Kronik, Fully numerical all-electron solutions of the optimized effective potential equation for diatomic molecules, J. Chem. Theory Comput. **5**, 1731 (2009).

[68] The DARSEC grid does not reach the $z$ axis exactly due to the use of prolate spheroidal coordinates, but one can use an elliptical line very close to the $z$ axis.

[69] In the light of footnote [64], this criterion is in line with the more direct observation noted in the Supplemental Material of Ref. [28].

[70] T. Aschebrock, T. Lebeda, M. Brütting, R. Richter, I. Schelter, and S. Kümmel, Exact exchange-like electric response from a meta-generalized gradient approximation: A semilocal realization of ultranonlocality, J. Chem. Phys. **159**, 234107 (2023).

[71] V. R. Cooper, Van der Waals density functional: An appropriate exchange functional, Phys. Rev. B **81**, 161104(R) (2010).

[72] Note that the energy factor in the original definition of the WTMAD-2 has been updated to 57.816 due to a correction of the MB16-43 average energy.

[73] T. Lebeda, T. Aschebrock, and S. Kümmel, First steps towards achieving both ultranonlocality and a reliable description of electronic binding in a meta-generalized gradient approximation, Phys. Rev. Res. **4**, 023061 (2022).

[74] S. Ehlert, U. Huniar, J. Ning, J. W. Furness, J. Sun, A. D. Kaplan, J. P. Perdew, and J. G. Brandenburg, r$^2$SCAN-D4: Dispersion corrected meta-generalized gradient approximation for general chemical applications, J. Chem. Phys. **154**, 061101 (2021).

[75] A. Najibi and L. Goerigk, The nonlocal kernel in van der Waals density functionals as an additive correction: An extensive analysis with special emphasis on the B97M-V and $\omega$B97M-V approaches, J. Chem. Theory Comput. **14**, 5725 (2018).

[76] J. Ning, M. Kothakonda, J. W. Furness, A. D. Kaplan, S. Ehlert, J. G. Brandenburg, J. P. Perdew, and J. Sun, Workhorse minimally empirical dispersion-corrected density functional with tests for weakly bound systems: r$^2$SCAN + RVV 10, Phys. Rev. B **106**, 075422 (2022).

[77] S. Grimme, A. Hansen, S. Ehlert, and J.-M. Mewes, r$^2$SCAN-3c: A "Swiss army knife" composite electronic-structure method, J. Chem. Phys. **154**, 064103 (2021).

[78] A. Najibi and L. Goerigk, DFT-D4 counterparts of leading meta-generalized-gradient approximation and hybrid density functionals for energetics and geometries, J. Comput. Chem. **41**, 2562 (2020).

[79] M. Korth and S. Grimme, "Mindless" DFT benchmarking, J. Chem. Theory Comput. **5**, 993 (2009).

[80] T. Gould, B. Chan, S. G. Dale, and S. Vuckovic, Identifying and embedding transferability in data-driven representations of chemical space, Chem. Sci. **15**, 11122 (2024).

[81] J. P. Perdew, A. Ruzsinszky, G. I. Csonka, L. A. Constantin, and J. Sun, Workhorse semilocal density functional for condensed matter physics and quantum chemistry, Phys. Rev. Lett. **103**, 026403 (2009).

[82] J. W. Furness, A. D. Kaplan, J. Ning, J. P. Perdew, and J. Sun, Accurate and numerically efficient r$^2$SCAN meta-generalized gradient approximation, J. Phys. Chem. Lett. **11**, 8208 (2020).

[83] J. W. Furness, A. D. Kaplan, J. Ning, J. P. Perdew, and J. Sun, Construction of meta-GGA functionals through restoration of exact constraint adherence to regularized SCAN functionals, J. Chem. Phys. **156**, 034109 (2022).

[84] A. D. Kaplan, M. Levy, and J. P. Perdew, The predictive power of exact constraints and appropriate norms in density functional theory, Annu. Rev. Phys. Chem. **74**, 193 (2023).

[85] M. G. Medvedev, I. S. Bushmarinov, J. Sun, J. P. Perdew, and K. A. Lyssenko, Density functional theory is straying from the path toward the exact functional, Science **355**, 49 (2017); K. P. Kepp, Comment on "density functional theory is straying from the path toward the exact functional", *ibid.* **356**, 496 (2017); M. G. Medvedev, I. S. Bushmarinov, J. Sun, J. P. Perdew, and K. A. Lyssenko, Response to comment on "density functional theory is straying from the path toward the exact functional", *ibid.* **356**, 496 (2017).

[86] Similarly, one could argue that even choosing a particular function is empirical, such as choosing to fulfill the gradient expansion by $(1+At^2)/(1+At^2+A^2t^4)$ in PBE correlation versus $(1+4At^2)^{-1/4}$ in SCAN correlation.

[87] P. Jurečka, J. Šponer, J. Černỳ, and P. Hobza, Benchmark database of accurate (MP2 and CCSD(T) complete basis set limit) interaction energies of small model complexes, DNA base pairs, and amino acid pairs, Phys. Chem. Chem. Phys. **8**, 1985 (2006).

[88] M. S. Marshall, L. A. Burns, and C. D. Sherrill, Basis set convergence of the coupled-cluster correction, $\delta_{\mathrm{MP2}}^{\mathrm{CCSD}(T)}$: Best practices for benchmarking non-covalent interactions and the attendant revision of the S22, NBC10, HBC6, and HSG databases, J. Chem. Phys. **135**, 194102 (2011).

[89] J. Heyd, G. E. Scuseria, and M. Ernzerhof, Hybrid functionals based on a screened coulomb potential, J. Chem. Phys. **118**, 8207 (2003) [**124**, 219906 (2006)].

[90] A. V. Krukau, O. A. Vydrov, A. F. Izmaylov, and G. E. Scuseria, Influence of the exchange screening parameter on the performance of screened hybrid functionals, J. Chem. Phys. **125**, 224106 (2006).

[91] R. Peverati and D. G. Truhlar, Communication: A global hybrid generalized gradient approximation to the exchange-correlation

functional that satisfies the second-order density-gradient constraint and has broad applicability in chemistry, J. Chem. Phys. **135**, 191102 (2011).

[92] R. Peverati and D. G. Truhlar, Quest for a universal density functional: the accuracy of density functionals across a broad spectrum of databases in chemistry and physics, Philos. Trans. R. Soc. A **372**, 20120476 (2014).

[93] J. Sun, M. Marsman, G. I. Csonka, A. Ruzsinszky, P. Hao, Y.-S. Kim, G. Kresse, and J. P. Perdew, Self-consistent meta-generalized gradient approximation within the projector-augmented-wave method, Phys. Rev. B **84**, 035117 (2011).

[94] R. Kingsbury, A. S. Gupta, C. J. Bartel, J. M. Munro, S. Dwaraknath, M. Horton, and K. A. Persson, Performance comparison of r$^2$SCAN and SCAN metaGGA density functionals for solid materials via an automated, high-throughput computational workflow, Phys. Rev. Mater. **6**, 013801 (2022).

[95] F. Hofmann, I. Schelter, and S. Kümmel, Molecular excitations from meta-generalized gradient approximations in the Kohn–Sham scheme, J. Chem. Phys. **153**, 114106 (2020).

[96] R. Richter, T. Aschebrock, I. Schelter, and S. Kümmel, Meta generalized gradient approximations in time dependent generalized Kohn Sham theory: Importance of the current-density correction, J. Chem. Phys. **159**, 124117 (2023).